Study of the Inhibition of Schumann Resonance-inspired Electromagnetic Field on Cancer Cell Proliferation

Xianqiang Yan[1], Xuelei Liu[3*], Shujun Zhang[1,2], Zhenning Liu[1*], Luquan Ren[1]

1. *Key Laboratory of Bionic Engineering (Ministry of Education), College of Biological and Agricultural Engineering, Jilin University, Changchun, 130022, China*
2. *School of Computing and Engineering, University of Gloucestershire, The Park, Cheltenham, GL50 2RH, UK*
3. *School of Mechanical Engineering, Shandong University of Technology, Zibo, 255000, China*

Abstract

Organisms on Earth evolve and coexist with natural Electromagnetic Fields (EMFs). Although many reports have suggested the potential anti-neoplastic effects of EMFs with specific parameters, the studies on the influence of natural EMFs on cancers are still rare. Herein, an EMF emitter has been developed to investigate the effects of the extremely-low frequency SR-mimicking EMF (SREMF) on cancer and normal cell proliferation. The numerical simulation has revealed that the emitter with specific parameters is able to enhance EMF intensity and uniformity on the designated plane above the emitter. More importantly, honeycomb-like emitter array can generate a stronger EMF intensity on the 20-mm plane above the array. Cell colony formation assays have demonstrated that SREMF generated by the honeycomb-like emitter array can significantly inhibit Hela cell proliferation in a cell-density-dependent manner. The morphological changes of SREMF-exposed Hela cells suggest that the anti-proliferative effect of SREMF may be caused by apoptosis induction. In contrast, no detrimental effect is observed for SREMF-treated normal cells, which probably can be explained by the evolutionary adaptation. Hence, this work can not only contribute to understanding the impact of natural EMF on creatures, but also afford a novel strategy to personalized cancer prevention and treatment.

Keywords: Electromagnetic fields (EMFs), Schumann resonance, EMF emitter, Cancer, Cell proliferation

1 Introduction

Human and other creatures on Earth live in an environment with various Electromagnetic Fields (EMFs), including natural EMFs (*e.g.* geomagnetic field)[1, 2] and EMFs generated by man-made sources (such as electrical appliances and equipments). Although there are some studies on the effects of natural EMFs on human health, the efforts are mainly sporadic and the conclusions are based on limited theoretical foundations and practical applications. Schumann Resonance (SR) is one of the well-investigated natural electromagnetic phenomena, which was first reported by Winfried Otto Schumann in 1952[3-6]. SR is a global electromagnetic resonance produced in the atmosphere by lightning, which consists of a base frequency about 7.83 Hz and a series of derived frequencies at 14 Hz, 20 Hz, 26 Hz, 33 Hz, 39 Hz, 45 Hz, and 51 Hz[7]. As an inherent part of the geomagnetic environment, SR is widely believed to benefit lives on the earth[4, 5, 7, 8]. On one hand, substantial frequency overlap has been found between SR bands and human brain waves, implying that human brain may have evolved to adapt to SR[3, 9]. Additionally, it has been demonstrated that a weak EMF mimicking SR can shield the heart from oxidative stress and hypoxic conditions[4]. On the other hand, it is known that the base frequency of SR closely approximates the resonance frequency of calcium ions (Ca^{2+}) within some cancer cells[10-13]. Moreover, several studies have shown that the low-intensity EMFs with an operating frequency at 7.83 Hz can significantly inhibit the cancer cell proliferation, probably through the modulation of Ca^{2+} influx[13-15].

In recent decades, there has been growing interest in applying Electric Fields (EFs) and EMFs to treat some common diseases, such as cancer[15-17], diabetes[18, 19], skin wound healing[20, 21] and neurological diseases[22, 23], *etc*. In particular, abundant literature has demonstrated that EFs and EMFs of characteristic parameters hold a great potential for cancer treatment[2, 13, 14, 24-32]. In early studies, Kirson *et al* have reported that an intermediate-frequency alternating EF yields a disruptive effect on cancer cell replication by impeding spindle formation during mitosis[24-26]. Concurrently, Sara Crocetti *et al* have revealed that an EMF with an extremely low frequency of 20 Hz and intensity of 3 mT suppresses the proliferation of breast cancer cells (MCF-7 cells) via

the induction of DNA damage, while nonmalignant counterparts (MCF-10 cells) remain intact under the identical EMF exposure[27]. Furthermore, Buckner *et al* have shown that the inhibition of low-intensity EMF on cancer cells depends on the spatiotemporal characteristics and is transduced by cAMP and ERK signaling pathways[28, 29]. In a recent study, Mojdeh Barati *et al* have found that the exposure to extremely-low frequency EMF can induce necroptosis (a kind of programmed cell death) in breast duct carcinoma cells (MC4-L2 cells) by ROS accumulation and Ca^{2+} overload[33]. In addition, some studies have reported that EMFs of specific parameters can render cancer cells more sensitive to chemotherapy, thus increasing the efficacy of chemotherapeutic drugs[30-32]. Collectively, these works underscore the multifaceted potential of EF and EMF therapies in reshaping cancer treatment strategies.

Previously, our group has demonstrated that a Bio-inspired EMF (BIEMF) can inhibit the proliferation of HeLa cells (human cervical adenocarcinoma cells) in a cell density-dependent manner[34]. The BIEMF used in our previous work has an extremely-low frequency of 0.5 Hz, which is chosen based on the inherent vibrational frequency observed in certain cancer cells[35]. In this work, we intend to investigate the effects of extremely-low frequency SR-mimicking EMF (SREMF) on cancer cell proliferation. Unfortunately, the EMF emitter used in our previous work, Magnafield (Model MF2200), is large in size and can only generate EMF with several fixed frequencies[34]. Other EMF emitters currently used in bioelectromagnetic studies, such as Solenoid coils [36-39] and Helmholtz coils[40-44], are also too big to fit in wearable devices. Hence, we have designed a honeycomb-like emitter array that not only can generate EMFs with adjustable frequencies and uniform distribution, but also holds a potential application in wearable devices. Then, a series of cell culture experiments have been conducted to examine the effects of SREMF on the proliferation of cancer and normal cells, which may offer valuable insights to the application of natural EMFs for cancer prevention and treatment.

2 Materials and Methods

2.1 Emitter Design and SREMF Irradiation System

2.1.1 Emitter Design by EMF Simulation

Maxwell 3D module of ANSYS Electronics Desktop was employed for numerical analysis of the EMFs generated by single emitters and emitter array. The parameters for EMF simulation are presented in Table 1. The simulation process of single emitter is as follows. First, an emitter model was constructed as a hollow cylinder with a thickness of 3 mm and a cuboid with air properties was set as the solving domain. Grid systems with maximum side lengths of 0.5 mm and 5 mm were set for the emitter and solving domain respectively to ensure the accuracy and reliability of the simulation. The current used in the windings of the emitter was a square-wave current with an amplitude of 0.7 A and a frequency of 0.5 Hz. Therefore, the simulation period was set as 2 s with a calculation step of 0.1 s. Then, the model was validated with the set parameters and the EMF distribution on the plane 20 mm above the emitter was analyzed.

Table 1 Parameters for EMF simulation

Parameters	Value	Unit
Length of solving domain	50	mm
Width of solving domain	50	mm
Height of solving domain	75	mm
Amplitude of input current	0.7	A
Frequency of input current	0.5	Hz
Maximum side length of grid for emitter	0.5	mm
Maximum side length of grid for solving domain	5	mm
Simulation period	2	s
Calculation step	0.1	s

2.1.2 SREMF Irradiation System Setup

The SREMF irradiation system consists of a signal generator, a power amplifier, an oscilloscope, a resistor and an emitter array, as shown in Fig. 1. The signal generator (Unit UTG2062B) can generate various electric waves within the frequency range of 1 μHz to 60 MHz from two independent channels. Nevertheless, the power provided by the signal generator is insufficient to drive the emitter array to generate an EMF of the

desired intensity. Hence, an amplifier (FeelTech, FPA2000-50W) with dual channels was chosen to amplify the voltage produced by the signal generator by 10 folds to drive the emitter array to generate SREMF. An oscilloscope (Unit UPO2102CS) was employed to monitor the voltage of the irradiation system in real time. Meanwhile, a resistor was used to protect the amplifier. The emitter array was mounted in the incubator for cell culture. Notably, cell culture dishes were placed on an acrylic plate about 2.5 cm above the emitter array and a thermal insulation layer made of polyurethane was inserted between the emitter array and the acrylic plate to prevent the heat effect of emitters on cells.

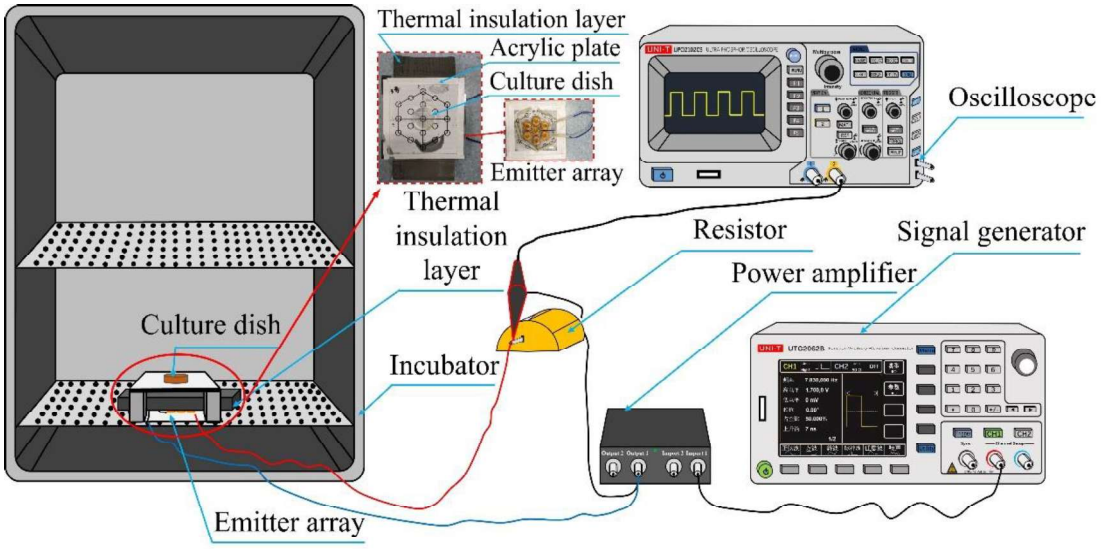

Fig. 1 Schematic illustration of SREMF irradiation system (the pictures show the top view of a culture dish placed above the emitter array and the underlying emitter array)

2.1.3 EMF Intensity Measurement

In order to validate the reliability of the simulation results, the EMF intensities at a series of designated points were measured with a Tesla meter probe (TianHeng TD8650 ± 0.5%) affixed to a vertical vernier caliper. First, two same pictures marked with points for EMF intensity measurement and emitter locations were respectively pasted on the same positions of two identical acrylic plates. Then, the emitters were affixed to the marked position on the picture on one of the acrylic plates. Next, the acrylic plate with the emitters was placed horizontally and another was supported at the 20 mm directly above this acrylic plate. Finally, EMF intensities at a series of marked

points on the upper acrylic plate were determined through horizontal movement of the probe.

2.2 Colony Formation Assay in Vitro

2.2.1 Cell Culture

Human cervical adenocarcinoma cells (Hela cells) were cultured in RPMI 1640 medium supplemented with 10% Fetal Bovine Serum (FBS, Gibco, USA) and 1% Penicillin-Streptomycin. Mouse fibroblast (NIH/3T3 cells) were cultured in Dulbecco's Modified Eagle Medium (DMEM) supplemented with 10% Newborn Bovine Serum (NBS, Gibco, USA) and 1% Penicillin-Streptomycin. The cells were maintained in an incubator (MCO-170AIVL-PC, Panasonic Healthcare, Japan) at a temperature of 37 °C with a humidified atmosphere of 5% CO_2.

2.2.2 SREMF Exposure

Cells were counted and seeded in culture dishes of 35 mm in diameter for SREMF exposure. After 24 hours of cell seeding, the culture dishes were placed on the acrylic plates about 2.5 cm above the SREMF emitter arrays. Each culture dish was exposed to an individual emitter array to ensure the same SREMF for all groups. Cells were subjected to continuous SREMF exposure for 6 days. Meanwhile, the non-exposed control dishes were kept at the otherwise same condition but without SREMF. The cell morphology of exposed and non-exposed groups was photographed every 2 days with a microscope (IX83, Olympus, Japan). The culture medium was refreshed every 2 days.

2.2.3 Crystal Violet Staining

Crystal violet staining was used to stain cell colonies of exposed and non-exposed groups after SREMF treatment as previously described[34]. Briefly, the culture medium was removed from the culture dishes and the cells were fixed with 4% paraformaldehyde for 15 to 30 minutes. Then, the cells were incubated with the crystal violet staining solution (Beyotime, China) for 15 minutes at room temperature after two washes with deionized water. Finally, the culture dishes were rinsed three times with deionized water, air-dried at room temperature, and then photographed. The images of

stained colonies were quantified by ImageJ software.

2.2.4 Statistical Analysis

Data of colony formation assay are presented as mean ± Standard Deviation (SD). Statistical significance was determined by one factor two-side t-test as previously described[34] and is denoted as *: $P < 0.05$, **: $P < 0.01$, ***: $P < 0.001$.

3 Results and Discussion

3.1 Emitter Design

3.1.1 Design of Single EMF Emitter

We have designed a ring-shaped EMF emitter based on the principle that circular circuit will generate EMF. The EMF emitter consists of 5 layers of enameled copper wire with a diameter of 0.6 mm, corresponding to a thickness of 3 mm. Then, nine emitters (Case1-9) with different inner and outer diameters have been designed with a fixed thickness of 3 mm to investigate the effects of ring diameters and number of turns on EMF intensity and uniformity. The detailed parameters of the nine emitters are shown in Table 2.

Then, the Maxwell 3D module of ANSYS Electronics Desktop was employed to simulate the EMFs generated by the emitters (Case 1-9). A comparative study of EMF distributions on 20 mm plane above the emitters was conducted to identify an emitter with the optimal performance in EMF generation. The schematic illustration of 20 mm plane above the emitter is shown in Fig. 2a. First, the overall EMF distribution of Case 1-9 on the 20-mm plane (Fig. 2b-2j) was evaluated. It is obvious that EMF intensity exhibits a radial gradual attenuation from the emitter center towards the periphery. As expected, the intensity of EMF is enhanced as the number of turns increases (and thus the outer diameter also increases) at the same inner diameter, while the uniformity decreases. To assess the uniformity of the EMFs, the EMF intensities at the point (0,0,20) 20 mm right above the emitter surface center (0,0,0) and the point on the 20-mm plane corresponding to the outer edge of the emitter are retrieved and denoted as B_0 and B_a respectively (Table 3). The ratio of relative EMF decline from the center to the edge was calculated as $(B_0\text{-}B_a)/B_0 \times 100\%$. It is found that B_0s of Cases 1, 4, 7 and 8 are below 90 μT, whereas the Cases 3, 6 and 9 display a larger ratio of EMF intensity decline

around 29%. Cases 2 and 5 are comparable, both yielding B_0 greater than 90 μT and a decline about 26%. Since Case 5 is relatively more uniform than Case 2, Case 5 is chosen as the emitter to build emitter arrays.

Table 2 Parameters of the designed EMF emitters

Case	Inner diameter (mm)	Outer diameter (mm)	Number of turns
1	5.6	17.6	50
2		20	60
3		22.4	70
4	8	17.6	40
5		20	50
6		22.4	60
7	10.4	17.6	30
8		20	40
9		22.4	50

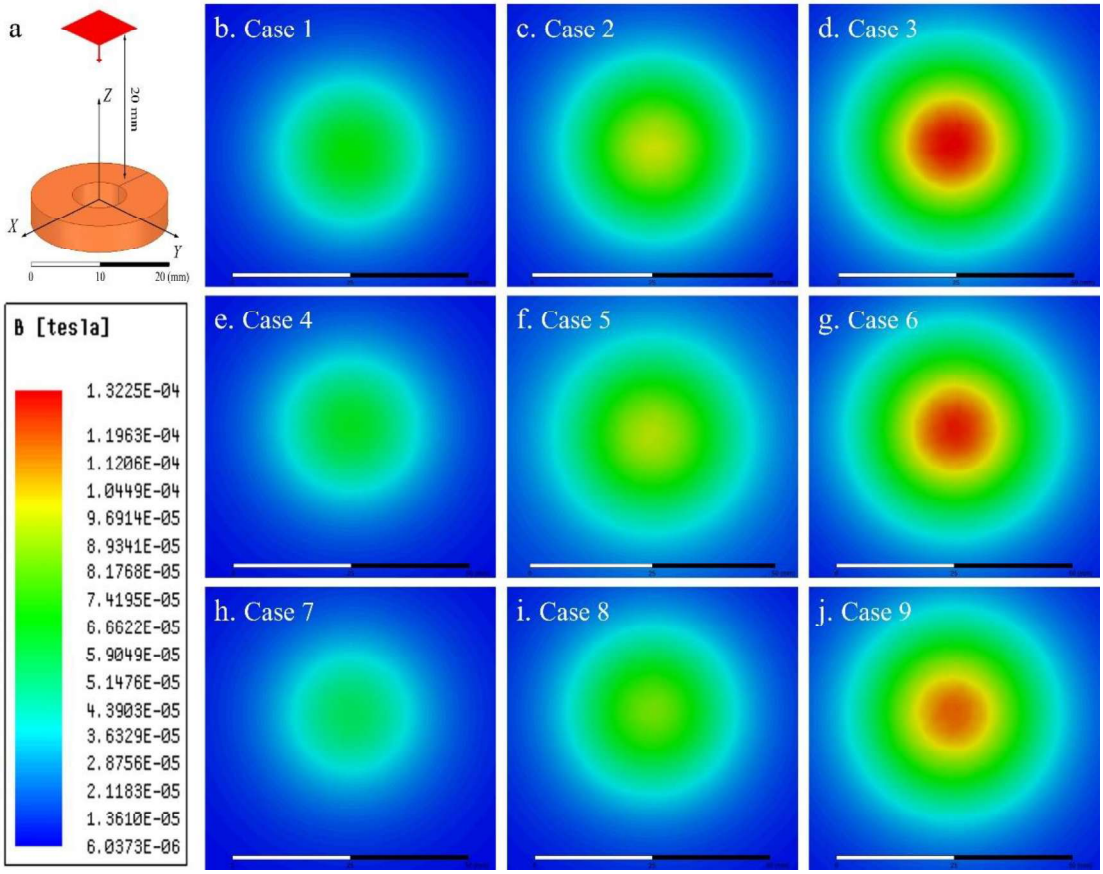

Fig. 2 EMF distribution on the 20-mm plane for Case 1-9. **a)** Schematic illustration of the 20-mm plane above the emitter surface. **b-j)** EMF distribution on the 20-mm plane for Case 1 to Case 9.

Table 3 The ratio of EMF intensity decline on the 20-mm plane

Case	B_0 (μT)	B_a (μT)	$B_0 - B_a$ (μT)	$(B_0\text{-}B_a)/B_0$
1	67.73	54.22	13.51	19.9%
2	96.97	72.00	24.97	25.8%
3	131.67	93.15	38.52	29.3%
4	63.00	49.10	13.90	22.1%
5	91.89	68.33	23.56	25.6%
6	127.94	90.18	37.76	29.5%
7	54.25	42.97	11.28	20.8%
8	83.90	62.44	21.46	25.6%
9	117.90	83.95	33.95	28.8%

3.1.2 Design of Emitter Array

Two kinds of emitter arrays have been designed, both of which can be tiled to fill a plane. One is a hexagon resembling a honeycomb and the other is a classic square (Fig. 3a and 3b). Six arrays with different emitter spacing (*S*) and thus different center-center distance (*d*) have been simulated and compared. The parameters of emitter arrays are presented in Table 4. As expected, the EMF intensities of emitter arrays are stronger than that of a single emitter at the same position relative to the emitter, indicating the superposition of EMFs generated by individual emitters (Fig. 3c-3h). Moreover, the EMF intensities of these two kinds of arrays decrease as *S* and *d* increase. It can be seen that hexagonal arrays are better than respective square arrays with the same *S* and *d* in terms of EMF intensity on the 20-mm plane. More importantly, the hexagonal array with *d* of 23 mm (Array 1) affords stronger EMF intensity in a hexagon with a side length about 43 mm on the 20-mm plane (Fig. 3c). It should be noted the number of emitters can be adjusted according to the intended EMF irradiation area for a wearable device of EMF treatment.

Table 4 Parameters of the designed emitter arrays

	Array	*S* (mm)	*d* (mm)
Honeycomb array	1	3	23
	2	5	25
	3	7	27
Square array	4	3	23
	5	5	25
	6	7	27

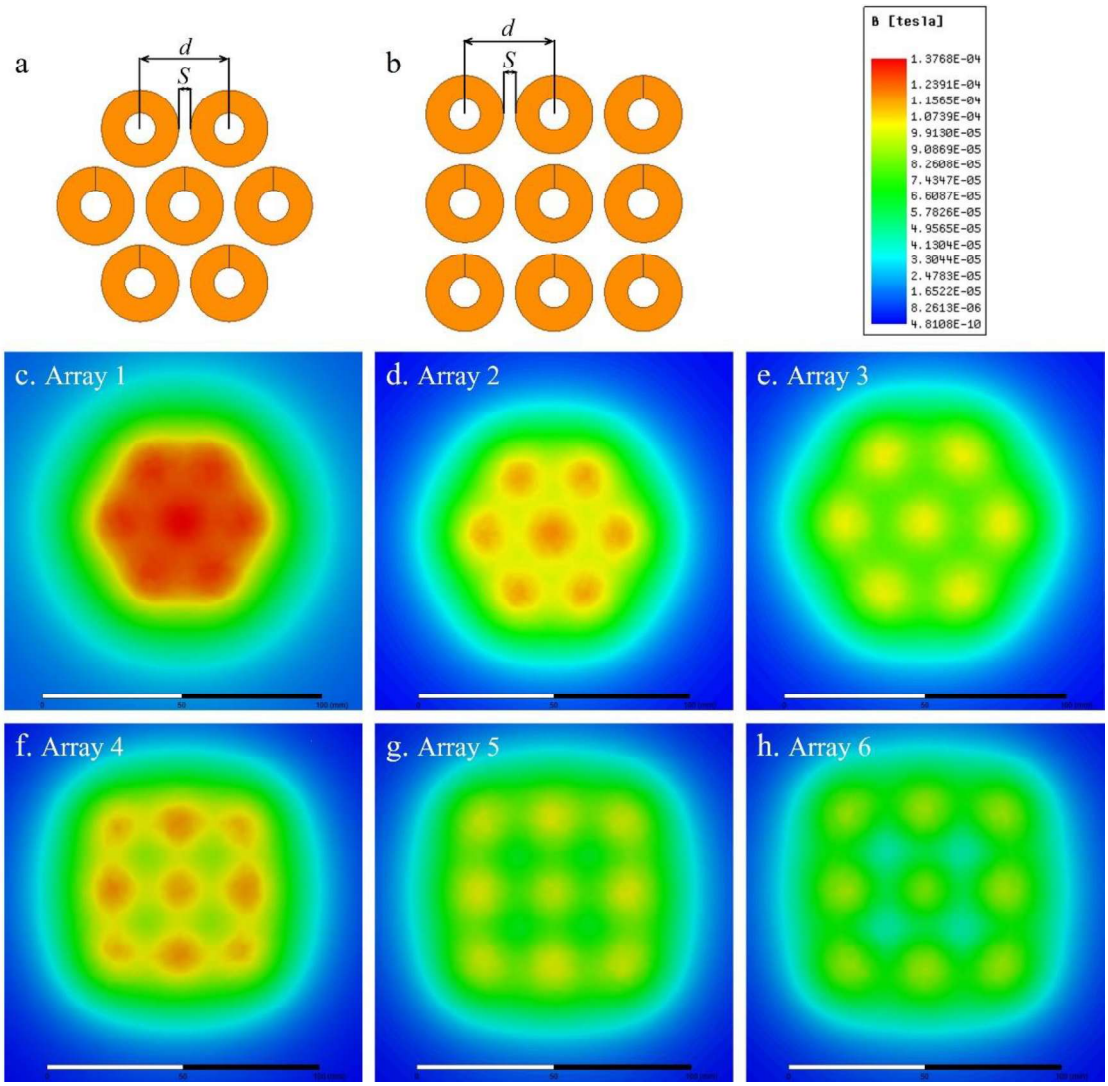

Fig. 3 EMF distribution on the 20-mm plane for Array 1-6. **a-b)** Schematic illustrations of the hexagonal and square arrays. **c-h)** EMF distribution on the 20-mm plane for Array 1 to Array 6.

3.1.3 Verification of Simulation Models

In this work, we have verified the simulation results by using a home-setup irradiation system as illustrated in Fig. 1. The SREMF was generated by an emitter driven by a square-wave voltage with an amplitude of 2.43 V at the frequency of 0.5 Hz (Fig. 4a). The amplitude generated by the signal generator was 0.78 V and the output voltage of the amplifier was 7.8 V, whereas the voltage on the emitter was 2.43 V due to the serial resistor. The EMF intensities on the lines from (0,-16,20) to (0,16,20) and from (0,-33,20) to (0,33,20) were measured for the single emitter (Case 5) and the emitter array (Array 1) respectively (Fig. 4b and Fig. 4c) and then compared with the

corresponding simulation results to validate the simulation models. For the single emitter, the measured EMF intensities and simulation results showed a similar trend, which decreased with the increase of the distance from the point (0,0,20) (Fig. 4d). Moreover, the deviations between the measured and simulated results increased with the distance from the point (0,0,20) and the maximum difference was 24.88%, which may be related to the winding errors of the emitter (Fig. 4d). For the emitter array, the EMF intensities acquired by measurement exhibited a roughly comparable trendline as the simulation results. However, the measured EMF intensities were stronger within the range of -24-24 mm from the point (0,0,20) (Fig. 4e). The maximum deviation between the measured and simulated results was 46.11% at the edge of the emitter array, which may be attributed to the errors of winding and array arrangement (Fig. 4e). For subsequent cell experiments, cell culture dishes were placed within the range of -24-24 mm from the point (0,0,20). We have also measured the actual SREMF waveform produced by our emitter array and found that it remains the shape of square wave.

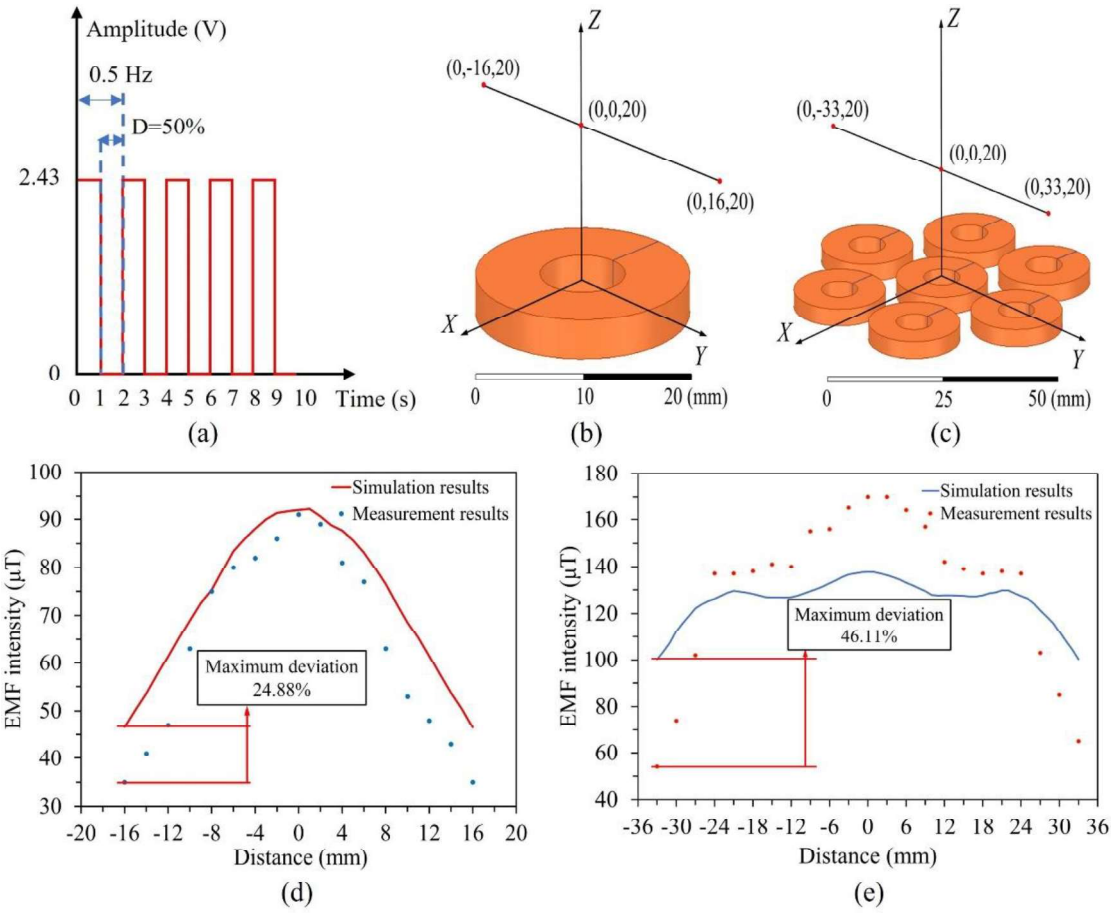

Fig. 4 Verification of SREMF intensity. **a)** The square-wave voltage to generate SREMF. b) Schematic illustration of the line from (0,-16,20) to (0,16,20) above the single emitter. **c)** Schematic illustration of the line from (0,-33,20) to (0,33,20) above the emitter array. **d)** EMF intensities of simulation and measurement on the line from (0,-16,20) to (0,16,20). **d)** EMF intensities of simulation and measurement on the line from (0,-33,20) to (0,33,20).

3.2 The Biological Effects of SREMF

3.2.1 The Effect of SREMF on Cancer Cell Proliferation

EMFs of varied frequencies may yield different biological effects, which is known as the "window effect" of frequency. It is well-documented that the resonance frequency of Ca^{2+} in some cancer cells is closed to 7.83 Hz[10-13]. Hence, the EMFs of specific intensity with the base frequency of SR can suppress the proliferation of cancer cells by modulating Ca^{2+} influx[13-15]. In addition, it has been previously demonstrated that EMF with intensities of around 200 μT and 600 μT can inhibit cancer cell proliferation[45, 46].

Inspired by the SR, we generated an SREMF at the frequency of 7.83 Hz with the hexagonal emitter array designed in this work (Array 1). The effect of SREMF of two intensities (200 μT and 600 μT, actual intensities measured by a Tesla meter) on cancer cell proliferation was investigated *via* colony formation assay with Hela cells. After 6-day SREMF exposure, cell colonies were examined by crystal violet staining. Interestingly, the SREMF inhibits colony formation of Hela cells in a cell-density-dependent manner (Fig. 5). At low cell density (100 cells/dish), no cell colony could be found in SREMF-exposed groups, while several colonies were formed in the non-exposed controls. When the cell seeding densities were raised to 500 and 5000 cells/dish, these was still no cell colony formed in the group treated with SREMF of 600 μT, while a few colonies could be seen in the 200 μT-treated group. As for the cells seeded at 10000 and 20000 per dish, colonies could be observed in both exposed groups after 6 days, but their numbers are significantly less than that of the non-exposed group. Moreover, fewer colonies could be found in the group exposed to SREMF of 600 μT

compared with that of the 200 μT-treated group. Previously, we have reported that a BIEMF of 0.5 Hz inhibits Hela cell proliferation in a cell-density-dependent manner, which could be explained by some collective antagonistic response evoked at higher cell density[34]. Notably, such an inhibitory effect of BIEMF disappeared for the cell seeding density beyond 3000 cells/dish. Although the inhibition of SREMF on Hela cell proliferation also diminishes as the cell density increases, the inhibition by SREMF persists at higher cell seeding densities. Indeed, SREMF demonstrates more than 50% inhibition on Hela cells even at the density of 20000 cells/dish (Fig. 5b). Hence, our recent results suggest a stronger inhibitory effect of SREMF (7.83 Hz) than BIEMF (0.5 Hz).

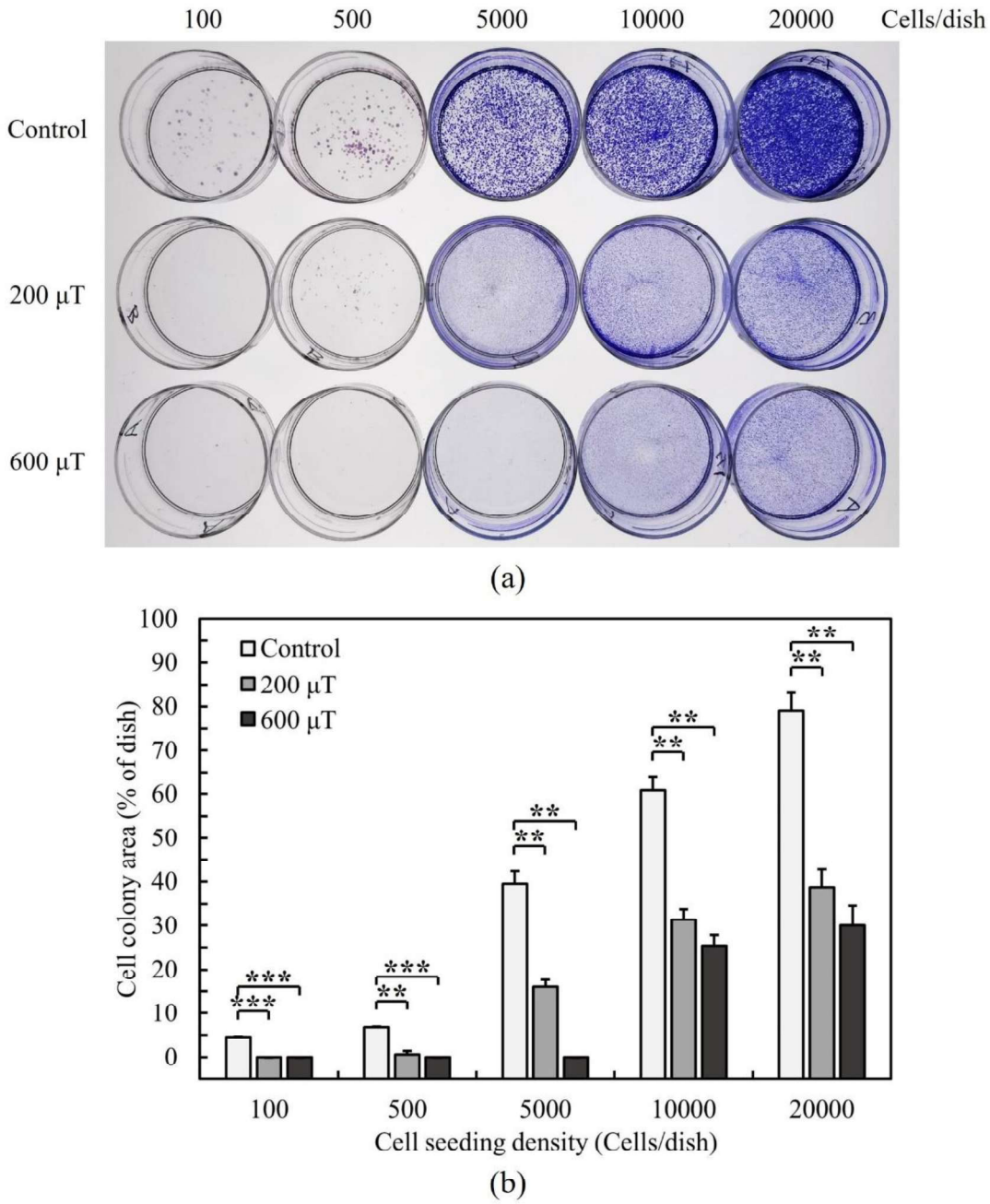

Fig. 5 Colony formation of Hela cells at the seeding densities ranging from 100 to 20000 cells/dish. **a)** Representative photographs of cell colony formation. **b)** Cell colony area as a percentage of the dish area. (**: $P < 0.01$, ***: $P < 0.001$)

It is known that the process of cell death is generally accompanied by changes in cellular morphology[47, 48]. Hence, we have examined Hela cell morphology during the 6 days of exposure at 2-day interval to verify the suppression by SREMF on Hela cells at the seeding density of 20000 cells/dish (Fig. 6). Compared to the non-exposed group,

no obvious morphology change was observed for the exposed groups after 2-day SREMF exposure (Fig. 6a, 6d and 6g). In contrast, after 4 days of SREMF exposure, some cells of the exposed groups exhibit obvious morphological changes with a few cells showing signs of early-stage death (Fig. 6e and 6h). After 6-day SREMF exposure, cells of the exposed group show more dramatic morphological changes of shrinkage, blebbing and fragmentation (Fig. 6f and 6i), whereas Hela cells of the control group have formed healthy foci (Fig. 6c). These observations have confirmed the inhibition of SREMF on Hela cell proliferation at the seeding density of 20000 cells/dish. More importantly, since the progression of swelling and shrinkage to blebbing in cell morphology is a known hallmark of apoptosis[47, 48], these results also suggest that the inhibition of SREMF may be mediated by the induction of apoptosis. Nonetheless, the exact mechanisms underlying SREMF-induced apoptosis of cancer cells warrant further investigation.

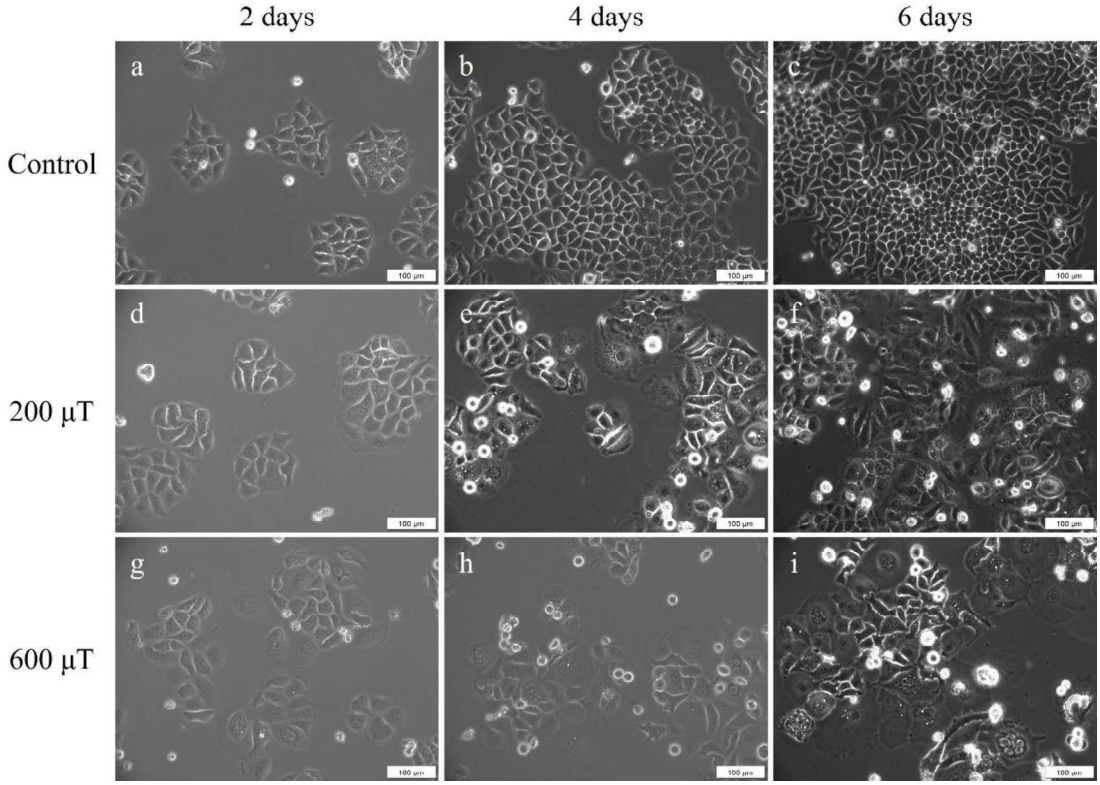

Fig. 6 The morphology of Hela cells without and with 6-day SREMF exposure. **a-c)** without SREMF, **d-f)** with SREMF of 200 μT, **g-i)** with SREMF of 600 μT. (Seeding density: 20000 cells/dish)

3.2.2 The Effect of SREMF on Normal Cell Proliferation

In order to determine whether the inhibition by SREMF is specific to cancer cells, we have also studied the proliferation of normal cells, *i.e.* NIH/3T3 cells, subjected to SREMF of 200 μT and 600 μT. As described above for Hela cells, crystal violet staining was conducted to examine the colony formation of NIH/3T3 cells after SREMF exposure of 6 days. As expected, no significant influence on colony formation was observed after 6-day SREMF exposure (Fig. 7). Specifically, at three cell seeding densities examined (500, 1000 and 5000 cells/dish), no significant difference in cell colonies was found between the exposed and non-exposed groups. We have also compared the morphology of NIH/3T3 cells with and without SREMF exposure at 2-day interval (Fig. 8). All cells appear to be healthy and no obvious difference in cell morphology could be found between the exposed and non-exposed groups. These results indicate that there is no detrimental effect of SREMF on normal cell growth. Yet it is not surprising since the frequency of SREMF (7.83 Hz) is consistent with the base frequency of SR, to which normal cells have adapted. In contrast, cancer cells may have gained distinctive characteristics during tumorigenesis and thus become susceptible to the frequency of SR.

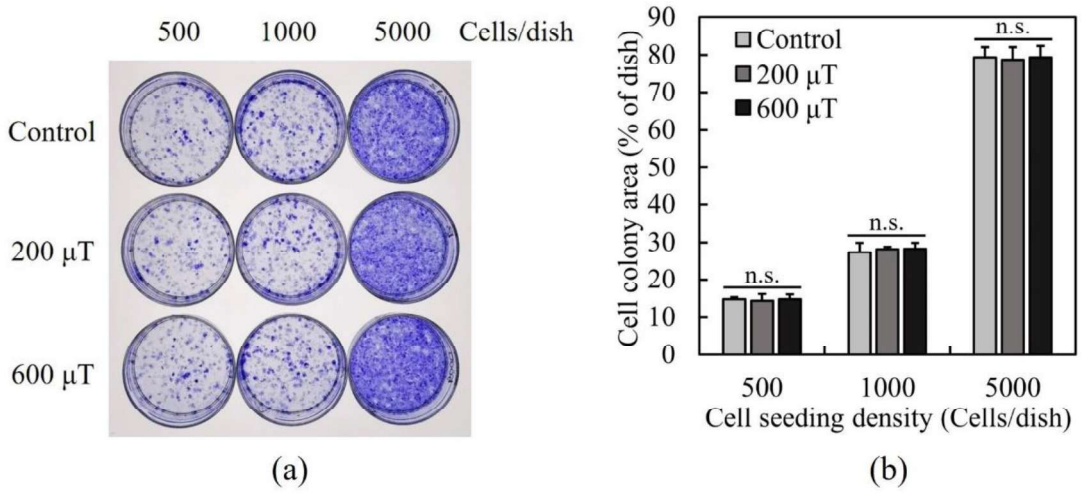

Fig. 7 Colony formation of NIH/3T3 cells at the seeding densities of 500, 1000 and 5000 cells/dish. **a)** Representative photographs of cell colony formation. **b)** Cell colony area as a percentage of the dish area. (n.s.: not significant)

.

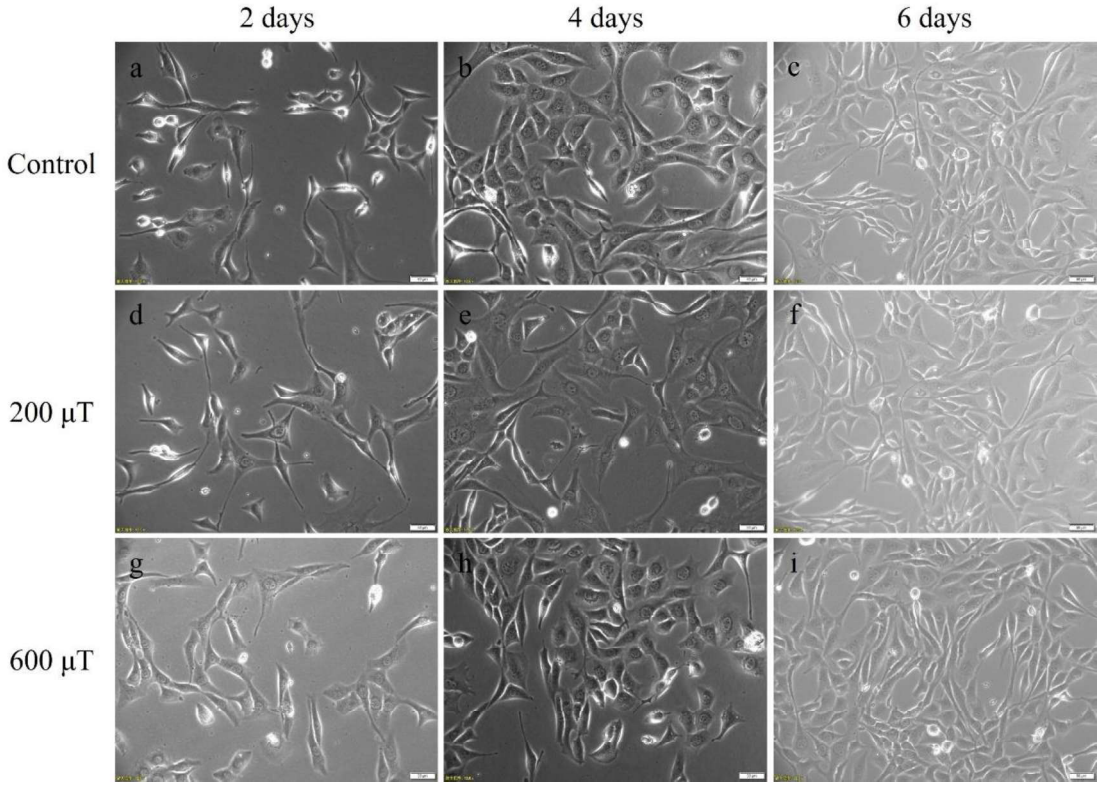

Fig 8 The morphology of NIH/3T3 cells without and with 6-day SREMF exposure. **a-c)** without SREMF, **d-f)** with SREMF of 200 μT, **g-i)** with SREMF of 600 μT. (Seeding density: 1000 cells/dish)

So far, it remains a mystery how weak Extremely-Low Frequency EMFs (ELF-EMFs) can cause biological effects[49-57]. The findings of the present study have demonstrated that the exposure to SREMF can significantly inhibit Hela cell proliferation, while exerting no observable effect on NIH/3T3 cells. Similar to our results, several studies have shown that low-intensity EMFs at a frequency near 7.83 Hz can hinder cancer cell growth[58-60]. One possible mechanism for such a phenomenon is through the modulation of Ca^{2+} influx. Intracellular Ca^{2+} plays an important role in cellular activities, such as apoptosis, proliferation and metabolism[61]. It has been reported that the resonance frequency of Ca^{2+} within certain cancer cells is close to the base frequency of SR[10-13]. Moreover, several studies have found the ELF-EMFs at 7.83 Hz can promote Ca^{2+} influx through modulating Ca^{2+}channels and thus cause cancer cell death due to intracellular Ca^{2+} overload[13-15] Another proposed mechanism is

mediated by Reactive Oxygen Species (ROS). Some studies have demonstrated that specific ELF-EMFs can significantly increase the level of intracellular ROS and induce DNA damage, resulting in cancer cell death[17, 27, 33, 62, 63]. However, the exact mechanism for the biological effects of ELF-EMFs, as well as for our SREMF, remains unclear, which warrants more in-depth investigation in the future.

4 Conclusions

In summary, we have developed an EMF emitter array to generate SREMF of extremely-low frequency (7.83 Hz) and then conducted cell experiments to investigate the effects of SREMF on cancer and normal cell proliferation. The numerical simulation has revealed that the emitter of Case 5 (inner diameter 8 mm, outer diameter 20 mm, 50 turns) can significantly improve the EMF intensity and uniformity on the designated plane above the emitter. More importantly, honeycomb-like emitter array is able to afford a stronger EMF intensity on the 20-mm plane above the array. The colony formation assay with Hela cells has demonstrated that SREMF generated by the honeycomb-like emitter array inhibits cancer cell proliferation in a cell-density-dependent manner. The morphological changes of SREMF-exposed Hela cells suggest that the anti-proliferative effect of SREMF may be caused by apoptosis induction. As expected, there is no detrimental effect of SREMF on the growth of normal cells, which probably can be explained by the evolutionary adaptation. Hence, our work can not only contribute to understanding the impact of geomagnetic environment on creatures, but also afford a novel strategy to personalized cancer prevention and treatment.

Conflict of Interest

On behalf of all authors, the corresponding author states that there is no conflict of interest.

Data Availability

The data that support the findings of this study are available from the corresponding author upon reasonable request.

Acknowledgement

This work was supported by National Key R&D Program of China (No. 2022YFE0138500) and Program of Jilin University Science and Technology Innovative Research Team (2020TD-03) and Natural Science Foundation of Shandong Province of China (ZR2022QE289).

References

[1] Thébault, E., Finlay, C. C., Beggan, C. D., Alken, P., Aubert, J., Barrois, O., Bertrand, F., Bondar, T., Boness, A., Brocco, L., Canet, E., Chambodut, A., Chulliat, A., Coïsson, P., Civet, F., Du, A., Fournier, A., Fratter, I., Gillet, N., Hamilton, B., Hamoudi, M., Hulot, G., Korte, M., Kuang, W., Lalanne, X., Langlais, B., Léger, J. M., Lesur, V., Lowes, F. J., Macmillan, S., Mandea, M., Manoj, C., Maus, S., Olsen, N., Petrov, V., Ridley, V., Rother, M., Sabaka, T. J., Saturnino, D., Schachtschneider, R., Sirol, O., Tangborn, A., Thomson, A., Toffner-Clausen, L., Vigneron, P., Wardinski, I., & Zvereva, T. (2015). International Geomagnetic Reference Field: the 12th generation. *Earth, Planets and Space*, *67*(1), 79.

[2] Liu, X. L., Yan, X. Q., Zhang, S. J., Liu, Z. N., Win, T. T. Y., & Ren, L. Q. (2021). The effects of electromagnetic fields on human health: Recent advances and future. *Journal of Bionic Engineering*, *18*(1), 210-237.

[3] Kozlowski, M., & Marciak-Kozlowska, J. (2015). Schumann resonance and brain waves: a quantum description. *NeuroQuantology*, *13*(2), 196-204.

[4] Elhalel, G., Price, C., Fixler, D., & Shainberg, A. (2019). Cardioprotection from stress conditions by weak magnetic fields in the Schumann Resonance band. *Scientific Reports*, *9*, 1645.

[5] Fdez-Arroyabe, P., Fornieles-Callejón, J., Santurtún, A., Szangolies, L., & Donner, R. V. (2020). Schumann resonance and cardiovascular hospital admission in the area of Granada, Spain: An event coincidence analysis approach. *Science of The Total Environment*, *705*, 135813.

[6] Schumann, W. O. (1952). Über die strahlungslosen Eigenschwingungen einer

leitenden Kugel, die von einer Luftschicht und einer Ionosphärenhülle umgeben ist. *Zeitschrift für Naturforschung A, A journal of Physical Sciences*, *7*(2), 149-154.

[7] Cherry, N. (2002). Schumann resonances, a plausible biophysical mechanism for the human health effects of solar/geomagnetic activity. *Natural Hazards*, *26*(3), 279-331.

[8] Cherry, N. (2003). Schumann resonance and sunspot relations to human health effects in Thailand. *Natural Hazards*, *29*(1), 1-11.

[9] Thomson, H. (2018). WAVE THERAPY. *Nature*, *555*(7694), 16-18.

[10] Lisi, A., Ledda, M., De Carlo, F., Foletti, A., Giuliani, L., D'Emilia, E., & Grimaldi, S. (2009). Calcium ion cyclotron resonance (ICR) transfers information to living systems: Effects on human epithelial cell differentiation. *Electromagnetic Biology and Medicine*, *27*(3), 230-240.

[11] Lisi, A., Ledda, M., De Carlo, F., Pozz, D., Messina, E., Gaetan, R., Chiment, I., Barile, L., Giacomell, A., D'Emilia, E., Giulian, L., Folett, A., Patt, A., Vulcan, A., & Grimaldi, S. (2008). Ion cyclotron resonance as a tool in regenerative medicine. *Electromagnetic Biology and Medicine*, *27*(2), 127-133.

[12] Panagopoulos, D. J., Karabarbounis, A., & Margaritis, L. H. (2002). Mechanism for action of electromagnetic fields on cells. *Biochemical and Biophysical Research Communications*, *298*(1), 95-102.

[13] Wang, M. H., Jian, M. W., Tai, Y. H., Jang, L. S., & Chen, C. H. (2021). Inhibition of B16F10 cancer cell growth by exposure to the square wave with 7.83+/-0.3Hz involves L- and T-type calcium channels. *Electromagnetic Biology and Medicine*, *40*(1), 150-157.

[14] Wang, M. H., Chen, K. W., Ni, D. X., Fang, H. J., Jang, L. S., & Chen, C. H. (2021). Effect of extremely low frequency electromagnetic field parameters on the proliferation of human breast cancer. *Electromagnetic Biology and Medicine*, *40*(3), 384-392.

[15] Tang, J. Y., Yeh, T. W., Huang, Y. T., Wang, M. H., & Jang, L. S. (2019). Effects of extremely low-frequency electromagnetic fields on B16F10 cancer cells.

Electromagnetic Biology and Medicine, *38*(2), 149-157.

[16] Costa, F. P., de Oliveira, A. C., Meirelles, R., Machado, M. C. C., Zanesco, T., Surjan, R., Chammas, M. C., Rocha, M. D., Morgan, D., Cantor, A., Zimmerman, J., Brezovich, I., Kuster, N., Barbault, A., & Pasche, B. (2011). Treatment of advanced hepatocellular carcinoma with very low levels of amplitude-modulated electromagnetic fields. *British Journal of Cancer*, *105*(5), 640-648.

[17] Yuan, L. Q., Wang, C., Lu, D. F., Zhao, X. D., Tan, L. H., & Chen, X. (2020). Induction of apoptosis and ferroptosis by a tumor suppressing magnetic field through ROS-mediated DNA damage. *Aging-US*, *12*(4), 3662-3681.

[18] Chen, Y. B., Li, J., Qi, Y. H., Miao, X., Zhou, Y. C., Ren, D.Q., & Guo, G. Z. (2010). The effects of electromagnetic pulses (EMP) on the bioactivity of insulin and a preliminary study of mechanism. *International Journal of Radiation Biology*, *86*(1), 22-26.

[19] Bahaoddini, A., Mohabatkar, H., Nikfarjam, M., & Keshtgar, S. (2011). Effect of exposure to low frequency electromagnetic field on the plasma glucose, insulin, triglyceride and cholesterol of male rats. *Journal of Applied Animal Research*, *34*(2), 179-180.

[20] Bai, W. F., Xu, W. C., Zhu, H. X., Huang, H., Wu, B., & Zhang, M. S. (2017). Efficacy of 50 Hz electromagnetic fields on human epidermal stem cell transplantation seeded in collagen sponge scaffolds for wound healing in a murine model. *Bioelectromagnetics*, *38*(3), 204-212.

[21] Costantini, E., Sinjari, B., D'Angelo, C., Murmura, G., Reale, M., & Caputi, S. (2019). Human gingival fibroblasts exposed to extremely low-frequency electromagnetic fields: in vitro model of wound-healing improvement. *International Journal of Molecular Sciences*, *20*(9), 2108.

[22] Podda, M. V., Leone, L., Barbati, S. A., Mastrodonato, A., Puma, D. D. L., Piacentini, R., & Grassi, C. (2014). Extremely low-frequency electromagnetic fields enhance the survival of newborn neurons in the mouse hippocampus. *European Journal of Neuroscience*, *39*(6), 893-903.

[23] Urnukhsaikhan, E., Mishig-Ochir, T., Kim, S. C., Park, J. K., & Seo, Y. K. (2017).

Neuroprotective effect of low frequency-pulsed electromagnetic fields in ischemic stroke. *Applied Biochemistry and Biotechnology*, *181*(4), 1360-1371.

[24] Kirson, E. D., Gurvich, Z., Schneiderman, R., Dekel, E., Itzhaki, A., Wasserman, Y., Schatzberger, R., & Palti, Y. (2004). Disruption of cancer cell replication by alternating electric fields. *Cancer Research*, *64*(9), 3288-3295.

[25] Kirson, E. D., Dbaly, V., Tovarys, F., Vymazal, J., Soustiel, J. F., Itzhaki, A., Mordechovich, D., Steinberg-Shapira, S., Gurvich, Z., Schneiderman, R., Wasserman, Y., Salzberg, M., Ryffel, B., Goldsher, D., Dekel, E., & Palti, Y. (2007). Alternating electric fields arrest cell proliferation in animal tumor models and human brain tumors. *Proceedings of the National Academy of Sciences of the United States of America*, *104*(24), 10152-10157.

[26] Kirson, E. D., Giladi, M., Gurvich, Z., Itzhaki, A., Mordechovich, D., Schneiderman, R. S., Wasserman, Y., Ryffel, B., Goldsher, D., & Palti, Y. (2009). Alternating electric fields (TTFields) inhibit metastatic spread of solid tumors to the lungs. *Clinical & Experimental Metastasis*, *26*(7), 633-640.

[27] Crocetti, S., Beyer, C., Schade, G., Egli, M., Fröhlich, J., & Franco-Obregón, A. (2013). Low intensity and frequency pulsed electromagnetic fields selectively impair breast cancer cell viability. *PLoS One*, *8*(9), e72944.

[28] Buckner, C. A., Buckner, A. L., Koren, S. A., Persinger, M. A., & Lafrenie, R. M. (2017). The effects of electromagnetic fields on B16-BL6 cells are dependent on their spatial and temporal character. *Bioelectromagnetics*, *38*(3), 165-174.

[29] Buckner, C. A., Buckner, A. L., Koren, S. A., Persinger, M. A., & Lafrenie, R. M. (2018). Exposure to a specific time-varying electromagnetic field inhibits cell proliferation via cAMP and ERK signaling in cancer cells. *Bioelectromagnetics*, *39*(3), 217-230.

[30] Baharara, J., Hosseini, N., & Farzin, T. R. (2016). Extremely low frequency electromagnetic field sensitizes cisplatin-resistant human ovarian adenocarcinoma cells via P53 activation. *Cytotechnology*, *68*(4), 1403-1413.

[31] Amiri, M., Basiri, M., Eskandary, H., Akbarnejad, Z., Esmaeeli, M., Masoumi-Ardakani, Y., & Ahmadi-Zeidabadi, M. (2018). Cytotoxicity of carboplatin on

human glioblastoma cells is reduced by the concomitant exposure to an extremely low-frequency electromagnetic field (50 Hz, 70 G). *Electromagnetic Biology and Medicine*, *37*(3), 138-145.

[32] Han, Q., Chen, R., Wang, F. J., Chen, S., Sun, X. S., Guan, X., Yang, Y., Peng, B. J., Pan, X. D., Li, J. F., Yi, W. J., Li, P., Zhang, H. W., Feng, D. F., Chen, A., Li, X. H., Li, S. H., & Yin, Z. M. (2018). Pre-exposure to 50 Hz-electromagnetic fields enhanced the antiproliferative efficacy of 5-fluorouracil in breast cancer MCF-7 cells. *Plos One*, *13*(4), e0192888.

[33] Barati, M., Javidi, M. A., Darvishi, B., Shariatpanahi, S. P., Moosavi, Z. S. M., Ghadirian, R., Khani, T., Sanati, H., Simaee, H., Barough, M. S., Farahmand, L., & Ansari, A. M. (2021). Necroptosis triggered by ROS accumulation and Ca^{2+} overload, partly explains the inflammatory responses and anti-cancer effects associated with 1Hz, 100 mT ELF-MF in vivo. *Free Radical Biology and Medicine*, *169*, 84-98.

[34] Liu, X. L., Liu, Z. M., Liu, Z. N., Zhang, S. J., Bechkoum, K., Clark, M., & Ren, L. Q. (2019). The effects of bio-inspired electromagnetic fields on normal and cancer cells. *Journal of Bionic Engineering*, *16*(5), 943-953.

[35] Meijer, D. K. F., & Geesink, H. J. H. (2018). Favourable and unfavourable EMF frequency patterns in cancer: Perspectives for improved therapy and prevention. *Journal of Cancer Therapy*, *9*(3), 188-230.

[36] Jia, H. L., Wang, C., Li, Y., Lu, Y., Wang, P. P., Pan, W. D., & Song, T. (2014). Combined effects of 50 Hz magnetic field and magnetic nanoparticles on the proliferation and apoptosis of PC12 Cells. *Biomedical and Environmental Sciences*, *27*(2), 97-105.

[37] Yang, W., Huo, X. L., & Song, T. (2008). Effects of extremely low-frequency-pulsed electromagnetic field on different-derived osteoblast-like cells. *Electromagnetic Biology and Medicine*, *27*(3), 298-311.

[38] Ahmadi-Zeidabadi, M., Akbarnejad, Z., Esmaeeli, M., Masoumi-Ardakani, Y., Mohammadipoor-Ghasemabad, L., & Eskandary, H. (2019). Impact of extremely low-frequency electromagnetic field (100 Hz, 100 G) exposure on human

glioblastoma U87 cells during Temozolomide administration. *Electromagnetic Biology and Medicine*, *38*(3), 198-209.

[39] Akbarnejad, Z., Eskandary, H., Vergallo, C., Nematollahi-Mahani, S. N., Dini, L., Darvishzadeh-Mahani, F., & Ahmadi, M. (2017). Effects of extremely low-frequency pulsed electromagnetic fields (ELF-PEMFs) on glioblastoma cells (U87) [J]. *Electromagnetic Biology and Medicine*, *36*(3), 238-247.

[40] Seze, R., Tuffet, S., Moreau, J. M., & Veyret, B. (2000). Effects of 100 mT time varying magnetic fields on the growth of tumors in mice. *Bioelectromagnetics*, *21*(2), 107-111.

[41] Diniz, P., Soejima, K., & Ito, G. (2002). Nitric oxide mediates the effects of pulsed electromagnetic field stimulation on the osteoblast proliferation and differentiation [J]. *Nitric Oxide-biology And Chemistry*, *7*(1), 18-23.

[42] Ventura, C., Maioli, M., Pintus, G., Gottardi, G., & Bersani, F. (2000). Elf-pulsed magnetic fields modulate opioid peptide gene expression in myocardial cells. *Cardiovascular Research*, *45*(4), 1054-1064.

[43] Xu, A. S., Wang, Q. A., & Lin, T. T. (2020). Low-frequency magnetic fields (LF-MFs) inhibit proliferation by triggering apoptosis and altering cell cycle distribution in breast cancer cells. *International Journal of Molecular Sciences*, *21*(8), 2952.

[44] Elexpuru-Zabaleta, M., Lazzarini, R., Tartaglione, M. F., Piva, F., Ciarapica, V., Busilacchi, E. M., Poloni, A., Valentino, M., Santarelli, L., & Bracci, M. (2023). A 50 Hz magnetic field influences the viability of breast cancer cells 96 h after exposure. *Molecular Biology Reports*, *50*(2), 1005-1017.

[45] Mahmoudinasab, H., Sanie-Jahromi, F., & Saadat, M. (2016). Effects of extremely low-frequency electromagnetic field on expression levels of some antioxidant genes in human MCF-7 cells. *Molecular biology research communications*, *5*(2), 77-85.

[46] Saliev, T., Begimbetova, D., Masoud, A. R., & Matkarimov, B. (2019). Biological effects of non-ionizing electromagnetic fields: Two sides of a coin. *Progress in Biophysics and Molecular Biology*, *141*, 25-36.

[47] Krysko, D. V., Vanden Berghe, T., D'Herde, K., & Vandenabeele, P. (2008). Apoptosis and necrosis: detection, discrimination and phagocytosis. *Methods*, *44*(3), 205-221.

[48] Kroemer, G., Galluzzi, L., Vandenabeele, P., Abrams, J., Alnemri, E. S., Baehrecke, E. H., Blagosklonny, M. V., El-Deiry, W. S., Golstein, P., Green, D. R., Hengartner, M., Knight, R. A., Kumar, S., Lipton, S. A., Malorni, W., Nuñez, G., Peter, M. E., Tschopp, J., Yuan, J., Piacentini, M., Zhivotovsky, B., & Melino, G. (2009). Classification of cell death: recommendations of the Nomenclature Committee on Cell Death 2009. *Cell Death And Differentiation*, *16*(1), 3-11.

[49] Silagadze, Z. K. (2021). Asteroid impact, Schumann resonances and the end of dinosaurs. *Physics Letters A*, *393*, 127156

[50] Karimi, A., Moghaddam, F. G., & Valipour, M. (2020). Insights in the biology of extremely low-frequency magnetic fields exposure on human health. *Molecular Biology Reports*, *47*(7), 5621-5633.

[51] Adey, W. R. (2013). The Energy around Us. *The Sciences*, *26*(1): 52-58.

[52] Funk, R. H. W., Monsees, T., & Özkucur, N. (2009). Electromagnetic effects – From cell biology to medicine. *Progress in Histochemistry and Cytochemistry*, *43*(4), 177-264.

[53] Binhi, V. N., & Savin, A. V. (2003). Effects of weak magnetic fields on biological systems: physical aspects. *Physics-Uspekhi*, *46*(3), 259-291.

[54] Adair, R. K. (1991). Constraints on biological effects of weak extremely-low-frequency electromagnetic fields. *Physical Review A*, *43*(2), 1039-48.

[55] Persinger, M. A., Ludwig, H. W., & Ossenkopp, K. P. (1973). Psychophysiological effects of extremely low frequency electromagnetic fields: A review. *Perceptual And Motor Skills*, *36*(3), 1131-1159.

[56] Ptitsyna, N. G., Villoresi, G., Dorman, L. I., Iucci, N., & Tyasto, M. I. (1998). Natural and man-made low-frequency magnetic fields as a potential health hazard. *Physics-Uspekh*, *41*(7), 687-709.

[57] Beers, G. J. (1989). Biological effects of weak electromagnetic fields from 0 Hz to 200 MHz: a survey of the literature with special emphasis on possible magnetic

resonance effects. *Magnetic Resonance Imaging*, *7*(3), 309-331.

[58] Makinistian, L., Marková, E., & Belyaev, I. (2019). A high throughput screening system of coils for ELF magnetic fields experiments: proof of concept on the proliferation of cancer cell lines. *BMC Cancer*, *19*, 188.

[59] Wang, T. T., Nie, Y. Z., Zhao, S. L., Han, Y. W., Du, Y. W., & Hou, Y. Y. (2011). Involvement of midkine expression in the inhibitory effects of low-frequency magnetic fields on cancer cells. *Bioelectromagnetics*, *32*(6), 443-452.

[60] Nie, Y. Z., Du, L. L., Mou, Y. B., Xu, Z. J., Weng, L. H., Du, Y. W., Zhu, Y. N., Hou, Y. Y., & Wang, T. T. (2013). Effect of low frequency magnetic fields on melanoma: tumor inhibition and immune modulation. BMC Cancer, 13, 582.

[61] Berridge, M. J. (2012). Calcium signalling remodelling and diseas. *Biochemical Society Transactions*, *40*(2), 297-309.

[62] Bergandi, L., Lucia, U., Grisolia, G., Granata, R., Gesmundo, I., Ponzetto, A., Paolucci, E., Borchiellini, R., Ghigo, E., & Silvagno, F. (2019). The extremely low frequency electromagnetic stimulation selective for cancer cells elicits growth arrest through a metabolic shift. *Biochimical et Biophysical Acta-molecular cell Research*, *1866*(9), 1389-1397.

[63] Yuan, L. Q., Wang, C., Lu, D. F., Zhao, X. D., Tan, L. H., & Chen, X. (2020). Induction of apoptosis and ferroptosis by a tumor suppressing magnetic field through ROS-mediated DNA damage. *Aging-US*, *12*(4), 3662-3681.